Submitted to

XXII International Symposium on Lepton-Photon Interactions at High Energy, June 30, 2005, Uppsala
Abstract: **406**
Sessions: **Flavor physics** and **QCD and hadron structure**

Photoproduction of Events Containing a $D^{*\pm}$ Meson and a Jet at HERA

H1 Collaboration

Abstract

Cross sections are measured for photoproduction events containing a $D^{*\pm}$ meson and a jet. The data were taken with the H1 detector at the ep collider HERA during the years 1999 and 2000. Photoproduction is selected by detecting the scattered positron at small angles. The cross sections are determined in the kinematic region $171 < W < 256$ GeV, $Q^2 < 0.01$ GeV^2, $p_t(D^*) > 2.0$ GeV and $|\eta(D^*)| < 1.5$, where W is the photon-proton centre-of-mass energy, Q^2 is the photon virtuality and p_t and η denote transverse momentum and pseudorapidity, respectively. Jets are defined by the inclusive k_t algorithm. The jet with the highest transverse momentum $p_t(jet) > 3$ GeV that does not contain the D^* meson is taken. Differential cross sections are shown as function of $p_t(jet)$, $p_t(D^*)$, $\eta(jet)$, $\eta(D^*)$ and of the azimuthal differences between the D^* and the jet, $\Delta\phi(D^*,\text{jet})$. The results are compared with perturbative QCD predictions in collinear and k_t-factorisation.

1 Introduction

The measurement of inclusive D^* photoproduction at HERA is interesting as a general test of the charm production mechanism in high energy ep collisions. The measurements [1–4] are consistent with the assumption that heavy quarks are predominantly produced via a photon-gluon fusion mechanism shown in figure 1.

The measurement of a D^*+jet pair gives the possibility to investigate further details of the charm production mechanism. The assumption is that the D^* meson and the jet approximate the kinematics of a charm or anti-charm quark and another parton, be it the other (anti-)charm, a light quark or a gluon.

Apart from single differential cross sections as a function of the transverse momenta and pseudorapidity of the D^* and the jet, measurements of observables of the D^*+jet system provide further stringent tests on the QCD calculations. The measurement of the difference in azimuthal angle $\Delta\phi(D^*,\text{jet})$ of the D^*+jet system is presented here. In photoproduction events the photon and the proton collide head-on. In collinear factorisation this applies also for the partons participating in the hard interaction. Therefore in a $2 \rightarrow 2$ process the azimuthal angle $\Delta\phi$ between the outgoing partons in the plane perpendicular to the incoming beams is exactly $180°$. Smaller $\Delta\phi$ can be due to additional (gluon) radiation and/or due to intrinsic transverse momenta k_t of the partons initiating the heavy quark production process. The measurement of $d\sigma/d\Delta\phi(D^*,\text{jet})$ provides thus a crucial test of the QCD calculation and the treatment of higher order QCD contributions. An illustrating sketch of the different contributions to the $\Delta\phi(D^*,\text{jet})$ distribution is shown in figure 2.

2 Data Selection

Data of the years 1999 and 2000 with an integrated luminosity of $\mathcal{L} = 51.1$ pb^{-1} are analysed where protons of $E_p = 920$ GeV have been collided with positrons of $E_e = 27.6$ GeV. The data selection is similar to the preliminary inclusive D^* measurement [3]. Tracks of charged particles are measured in the two Central Jet Chambers [5] placed concentrically around the beam line in a homogeneous magnetic field of 1.15 Tesla and covering the polar angular range[1] $20° < \theta < 160°$. The D^* meson is reconstructed via the decay channel[2] $D^{*+} \rightarrow D^0\pi_s^+ \rightarrow K^-\pi^+\pi_s^+$.

Photoproduction is selected through the reconstruction of the scattered positron in a crystal Čerenkov calorimeter close to the beam line 33 m away from the nominal interaction point, the electron tagger [6]. The small scattering angle $\pi - \theta_{e'} < 5$ mrad leads to the kinematic range of $Q^2 < 0.01$ GeV^2 and $0.29 < y < 0.65$ where the inelasticity y is reconstructed from the reconstructed positron energy $E_{e'}$, $y = 1 - E_{e'}/E_e$. The range in the inelasticity y corresponds to photon-proton centre-of-mass energies of $171 < W < 256$ GeV. Compared to [3] the transverse momentum cuts for the D^* and the kaon are lowered. The following criteria are applied to ensure good D^* reconstruction:

[1]The polar angle θ is measured with respect to the direction of the colliding protons.
[2]Charge conjugate states are always implicitly included.

- transverse momentum requirements for the D^* and its decay tracks of $p_t(D^*) > 2.0$ GeV, $p_t(K,\pi) > 0.3$ GeV and $p_t(\pi_s) > 0.12$ GeV,
- the application of particle identification using the specific energy loss dE/dx,
- a cut on the sum of the transverse momenta of the kaon and the pion from the D^0 decay, $p_t(K) + p_t(\pi) > 2.2$ GeV
- and the cut $p_t(D^*)/S_{E_t} > 0.10$, where S_{E_t} is the scalar sum of all reconstructed hadronic-final-state (HFS) objects with polar angle $\theta > 10°$, $S_{E_t} = \sum_{HFS}^{\theta>10°} \sin\theta_i E_i$.

Details can be found in [7].

Jets are defined by the inclusive k_t-algorithm [8] in the p_t-recombination and ΔR-distance scheme. The input of the jet algorithm are hadronic-final-state objects (HFS) from combining tracks reconstructed in the Central Jet Chamber and clusters in the calorimeters. The algorithm is run in the laboratory frame.

To ensure that all decay particles of the D^* candidate end up in the same jet, the HFS objects of the D^* decay tracks are replaced by the D^* candidate itself, i. e. the four-vectors that belong to the D^* decay tracks are replaced by the sum of the momenta of the tracks assigning the kaon and pion mass, respectively. In events which contain more than one D^* candidate, the jet algorithm is run separately for each candidate. For each candidate only its own decay tracks are replaced by the D^* candidate.

The minimal required transverse momentum is p_t(jet) > 3 GeV. To ensure a satisfying jet reconstruction even at these low values of p_t, jets are restricted to the central detector region $|\eta(\text{jet})| < 1.5$ where well measured tracks dominate the HFS objects.

The aim is to tag a second object besides the D^* from the hard process. Therefore jets *not* containing the D^* meson are selected. For about 50% of the inclusive D^* mesons at least one (non-D^*-)jet is found, for about 10% also a second such jet. If more than one (non-D^*-)jet is found, the jet with the highest transverse momentum is chosen. In total a signal of 588 ± 46 D^*+jet combinations is observed.

3 QCD Calculations

The results will be compared with two leading order calculations supplemented with parton showers, the collinear factorising PYTHIA 6.15 [9] and the k_t-factorising CASCADE 1.2 [10–12], as well as collinear next-to-leading (NLO) calculations in the massive (FMNR [13,14]) and massless (ZMVFNS [15,16]) scheme. In all calculations the charm mass is set to $m_c = 1.5$ GeV and the fragmentation fraction $f(c \to D^*) = 0.235$ [17] is applied.

For PYTHIA three different processes are generated separately and added afterwards: direct photon-gluon fusion, resolved processes with a light quark or a gluon from the photon and charm excitation processes where a charm quark from the photon enters the hard scatter. In the latter process the charm quark is treated as a massless parton like the light quarks whereas in the other processes the charm mass is accounted for in all steps of the calculation. Proton and photon density parameterisations CTEQ5L [18] and GRV-H LO [19] are used. Lund string fragmentation is applied as implemented in PYTHIA. For the longitudinal fragmentation of the charm quark into the D^* meson the Peterson parametrisation [20] is used with $\epsilon_{pet} = 0.078$. No uncertainties are determined for the PYTHIA prediction.

For the CASCADE calculations the renormalisation scale $\mu_r^2 = 4m_c^2 + p_t^2$ is chosen and the gluon density set A0 [21] is used. The fragmentation is treated as in PYTHIA. The importance of higher order terms is estimated by using the sets A0+ and A0- instead which apply the renormalisation scale multiplied and divided by two, respectively. Separately the charm mass has been varied from the default value $m_c = 1.5$ GeV to $m_c = 1.3$ and $m_c = 1.7$ GeV. The largest deviations of these four calculations from the default set define the upper and lower bound of the uncertainties of the CASCADE calculation. In most regions of phase space considered in this analysis the mass variations have the largest effect.

The main parameters of the (massive) FMNR and (massless) ZMVFNS calculations are listed in the tables 1 and 2. The massless scheme is expected to work well [22] for $p_t \gg m_c$ which is not always satisfied for the phase space considered here. On the other hand the massive scheme neglects terms $\propto \alpha_s \ln(p_t/m_c)$ and thus is expected not to be be accurate for high transverse momenta.

In the FMNR calculation the charm fragmentation is treated as longitudinal down scaling of the charm momentum according to the Peterson fragmentation function. The parameter $\epsilon_{pet} = 0.035$ is chosen [23]. The uncertainty of the cross section prediction has been estimated as follows: For each bin of the measurement the maximal deviation up- and downward obtained by individually varying the renormalisation scale, the factorisation scale, the charm mass and ϵ_{pet} as stated in table 1 define the upper and lower bound of the prediction.

ZMVFNS applies fragmentation functions determined in [24]. The uncertainty of the ZMVFNS calculation is estimated by considering the influence of varying the scales simultaneously in opposite directions as stated in table 2.

For both NLO calculations corrections are applied to account for the transition from parton level to hadron level jets. The corrections are calculated using PYTHIA. In PYTHIA parton level jets are constructed from the generated quarks and gluons after the parton showering step. The D^*-jet is identified as the jet containing the (anti-)charm quark which fragments into the D^*. The ratio of hadron and parton level cross sections in each bin is applied as hadronisation correction factor to the NLO calculations.

4 Cross Sections Determination

The bin averaged differential cross section in a variable Y is calculated according to

$$\frac{d\sigma_{vis}(ep \to e'D^*\text{+jet}X)}{dY} = \frac{N(D^*) \cdot (1-r)}{\Delta Y \cdot \mathcal{BR}(D^* \to K\pi\pi_s) \cdot \mathcal{L} \cdot \epsilon}. \qquad (1)$$

ΔY stands for the width of the considered bin and $N(D^*)$ is the number of D^* mesons associated with a jet in this bin, determined by a fit to the $\Delta m = m(K\pi\pi_s) - m(K\pi)$ distributions of the selected D^* candidates. The correction for reflections from other D^0 decays in the Δm distributions is denoted $(1-r) = 0.965$ [1,25], $\mathcal{BR}(D^* \to K\pi\pi_s) = 0.0257$ [26] is the branching ratio of the analysed D^* decay chain, $\mathcal{L}$ is the integrated luminosity and ϵ is the product of the track acceptance and reconstruction efficiency, of the efficiency of particle identification and triggering and of the electron tagger acceptance. The trigger and track efficiencies as well as the track acceptance have been determined using a GEANT 3 [27] based simulation, the remaining correction factors are deduced from data.

The main systematic uncertainties of the resulting cross sections are due to the uncertainty in the track reconstruction efficiency. Further relevant uncertainties arise from the determination of the electron tagger acceptance, the trigger uncertainty and the model dependence in the determination of the factors based on simulations. Quadratically adding the uncertainties of the different sources results in a total systematic uncertainty of 15-17% for each measured bin.

5 Results

The D^*+jet cross section as a function of $p_t(\text{jet})$ and $p_t(D^*)$ are shown in figure 3 and compared with predictions of PYTHIA, CASCADE, FMNR and ZMVFNS. Both distributions are rapidly falling towards higher transverse momenta and are reasonably well described by all QCD calculations, but the CASCADE prediction shows a slightly harder spectrum than observed in the data.

Cross sections as a function of the pseudorapidity of the jet and the D^*, respectively, are shown in figure 4. They differ noticeably: The $\eta(D^*)$ distribution falls off with increasing values of η (similar to the inclusive analysis) whereas $\eta(\text{jet})$ is almost flat. It has been checked that this difference is not caused by the slightly different kinematic cuts for the D^* and the jet, as can be seen from the direct PYTHIA distribution. The comparison of the $\eta(D^*)$ with the $\eta(\text{jet})$ cross sections suggests, that the jet cross section contains not only a charm jet in which case the D^* and the jet distributions would be expected to be similar. If, however, the jet cross section contains also contributions from hard gluon radiation from the initial state (such as included in a $\gamma g \to c\bar{c}g$ process), which tend to populate mainly the forward (large η) region, the behaviour of the measured cross section could be understood. This hypothesis is also supported from comparison with the QCD calculations, which show exactly this effect. For direct photon processes ($\gamma g \to c\bar{c}$) as simulated in PYTHIA (*dir.*), the η spectra of the jet and the D^* are found to be similar (figure 4 left), only after inclusion of the charm excitation processes, which effectively simulate processes like $\gamma g \to c\bar{c}g$, the η spectrum of the jet can be appropriately described. A similar feature is obtained with k_t factorisation as implemented in CASCADE, but also with the NLO calculations. The FMNR calculations describe the slopes reasonably well whereas in ZMVFNS especially $\eta(D^*)$ shows a steeper slope than the data.

In figure 5 the cross section is presented as a function of $\Delta\phi(D^*, \text{jet})$. It is interesting to observe, that only $\sim 25\%$ of the measured cross section come from a back-to-back configuration. Such a configuration would be observed if the dominant process would be $\gamma g \to c\bar{c}$. However, a large fraction of events where the D^* and the jet are not back-to-back suggest a significant contribution of higher order QCD radiation. In the DGLAP type event generator (PYTHIA) such contribution is simulated with the help of leading log parton showers, but also coming from the resolved photon processes and charm excitation. In the CASCADE calculation the $\Delta\phi(D^*, \text{jet})$ distribution is directly correlated with the k_t of the gluon generating the $c\bar{c}$ pair and therefore sensitive to the un-integrated gluon density.

In the NLO calculations $\Delta\phi(D^*, \text{jet}) \neq 180°$ comes entirely from real gluon emission and therefore the calculations are essentially LO for this observable. It is interesting to mention, that due to infrared sensitivity the NLO calculations (FMNR and ZMVFNS) give a huge negative cross section in the highest $\Delta\phi(D^*, \text{jet})$ bin which is compensated by a large positive contribution in the next lower $\Delta\phi(D^*, \text{jet})$ bin. Therefore both bins are averaged to be compared to the measurement. It is also interesting to observe, that the $\Delta\phi(D^*, \text{jet}) \approx 100°$ region is not described by the FMNR or ZMVFNS calculations indicating the sensitivity to even higher order contributions. Such higher order contributions could come from one or more partons radiated in the initial or final state. In CASCADE and PYTHIA these contributions are simulated with parton showers. It is still open whether resummations to all orders (as implemented in the parton shower approach) are needed or whether a parton level calculations of $\mathcal{O}(\alpha_s^3)$ is already sufficient to describe the measurements.

6 Conclusions

Photoproduction of D^* mesons has been analysed at relatively low transverse momenta. Cross sections have been determined for events with a D^* meson and a jet not containing the D^*. The results have been compared with four approaches of QCD calculations.

The measured transverse momentum distributions of the D^* and jet are in general in agreement with the prediction within the theoretical uncertainties.

Comparing the pseudorapidity distributions of the D^* and the jet it is striking that the $\eta(D^*)$ falls in forward direction whereas $\eta(\text{jet})$ is almost constant. This observation suggests that the jet cross section contains not only a charm jet but also a significant contribution form a further parton, most likely a gluon jet. The gluon radiation can be described by several approaches: By parton showers in combination with charm excitation processes (PYTHIA), an initial gluon ladder in k_t factorisation with initial state parton showers (CASCADE) or the presence of a gluon radiation in the hard process (NLO calculations).

The azimuthal difference $\Delta\phi(D^*, \text{jet})$ is sensitive to the amount of gluon radiation. The measured cross section shows, that only $\sim 25\%$ come from a LO process ($\gamma g \rightarrow c\bar{c}$) with a collinear gluon. The higher orders contribute significantly. The $\Delta\phi(D^*, \text{jet})$ is reasonably well described by calculations applying leading log parton showers in the collinear factorisation ansatz, or by using un-integrated gluon densities in the k_t-factorisation ansatz. It is interesting to observe, that the smaller $\Delta\phi(D^*, \text{jet})$ region is not described by the FMNR or ZMVFNS calculations indicating the sensitivity to even higher order contributions.

References

[1] C. Adloff, *et al.* (H1), Nucl. Phys., **B545**, (1999) 21. hep-ex/9812023.

[2] J. Abbiendi, *et al.* (ZEUS), Eur. Phys. J., **C6**, (1999) 67. hep-ex/9807008.

[3] H1, *Photoproduction of D^* Mesons at HERA*, International Europhysics Conference on High Energy Physics, EPS03, Aachen (2003). Abstract 097, H1prelim-03-071, URL http://www-h1.desy.de/h1/www/publications/htmlsplit/H1prelim-03-071.long.html.

[4] ZEUS, *Measurement of D^* Photoproduction at HERA*, 31st International Conference on High Energy Physics, ICHEP '02, Amsterdam (2002). Abstract 786, ZEUS-prel-02-004, URL http://www-zeus.desy.de/physics/phch/conf/amsterdam_paper.html.

[5] I. Abt, *et al.* (H1), Nucl. Instrum. Meth., **A386**, (1997) 348.

[6] I. Abt, *et al.* (H1), Nucl. Instrum. Meth., **A386**, (1997) 310.

[7] G. Flucke, *Photoproduction of D^* Mesons and D^* Mesons Associated with Jets at HERA*, Ph.D. thesis, Universität Hamburg (2005). DESY-THESIS-2005-006.

[8] S. Ellis, D. Soper, Phys. Rev., **D48**, (1993) 3160. hep-ph/9305266.

[9] T. Sjöstrand, *et al.*, Comput. Phys. Commun., **135**, (2001) 238. hep-ph/0010017.

[10] H. Jung, G. P. Salam, Eur. Phys. J., **C19**, (2001) 351. hep-ph/0012143.

[11] H. Jung, Comput. Phys. Commun., **143**, (2002) 100. hep-ph/0109102.

[12] H. Jung, *The CCFM Monte Carlo Generator CASCADE Version 1.2007* (2004). URL http://www.desy.de/~jung/cascade/cascade12007.ps.gz.

[13] S. Frixione, M. L. Mangano, P. Nason, G. Ridolfi, Phys. Lett., **B348**, (1995) 633. hep-ph/9412348.

[14] S. Frixione, P. Nason, G. Ridolfi, Nucl. Phys., **B454**, (1995) 3. hep-ph/9506226.

[15] G. Heinrich, B. A. Kniehl, Phys. Rev., **D70**, (2004) 094035. hep-ph/0409303.

[16] B. A. Kniehl, *in 14th Topical Conference on Hadron Collider Physics* (eds. M. Erdmann, T. Müller), 161–170 (Springer, Heidelberg, 2003). hep-ph/0211008.

[17] L. Gladilin, *Charm Hadron Production Fractions* (1999). hep-ex/9912064.

[18] H. L. Lai, *et al.* (CTEQ), Eur. Phys. J., **C12**, (2000) 375. hep-ph/9903282.

[19] M. Glück, E. Reya, A. Vogt, Phys. Rev., **D46**, (1992) 1973.

[20] C. Peterson, D. Schlatter, I. Schmitt, P. Zerwas, Phys. Rev., **D27**, (1983) 105.

[21] H. Jung, *in XII International Workshop on Deep Inelastic Scattering (DIS 2004)* (eds. D. Bruncko, J. Ferencei, P. Stríženec), vol. 1, 299–302 (SAS, 2004). `hep-ph/0411287`.

[22] W.-K. Tung, S. Kretzer, C. Schmidt, J. Phys., **G28**, (2002) 983. `hep-ph/0110247`.

[23] P. Nason, C. Oleari, Nucl. Phys., **B565**, (2000) 245. `hep-ph/9903541`.

[24] J. Binnewies, B. A. Kniehl, G. Kramer, Phys. Rev., **D58**, (1998) 014014. `hep-ph/9712482`.

[25] S. Hengstmann, *A Measurement of Diffractive Charm Production at HERA*, Ph.D. thesis, Universität Zürich (2000).

[26] S. Eidelman, *et al.* (Particle Data Group), Phys. Lett., **B592**, (2004) 1.

[27] R. Brun, *et al.*, *GEANT 3 User's Guide* (1987). `CERN-DD/EE/84-1`.

FMNR	μ_r	μ_f	m_c [GeV]	ϵ_{pet}	p-PDF	γ-PDF
decreasing σ	$2 \cdot m_t$	m_t	1.7	0.042		
default	m_t	$2 \cdot m_t$	1.5	0.035	CTEQ5M [18]	GRV-G HO [19]
increasing σ	$0.5 \cdot m_t$	$4 \cdot m_t$	1.3	0.028		

Table 1: *Renormalisation (μ_r) and factorisation (μ_f) scales, the charm pole mass (m_c), the Peterson parameters (ϵ_{pet}) and the parton density parametrisations of the D^* cross section calculations with the FMNR program with their default settings and variations. The transverse mass is defined as $m_t = \sqrt{m_c^2 + (p_{t,c}^2 + p_{t,\bar{c}}^2)}$.*

ZMVFNS	Fragmentation	μ_r	μ_f	p-PDF	γ-PDF
decreasing σ		$2 \cdot m_t$	$1.25 \cdot m_t$		
default	BKK O [24]	m_t	$2 \cdot m_t$	CTEQ5M [18]	GRV [19]
increasing σ		m_t	$4 \cdot m_t$		

Table 2: *Main parameters of the* ZMVFNS *next-to-leading order QCD calculation with their default settings and variations which lead to an increasing and decreasing prediction of the total visible cross section, respectively. The treatment of the charm fragmentation into D^* mesons, the factorisation and renormalisation scales μ_f and μ_r and the parton density parametrisations of the proton and the photon are given. The* transverse *mass is defined as $m_t = \sqrt{m_c^2 + p_t^2(D^*)}$ with the charm mass $m_c = 1.5$* GeV.

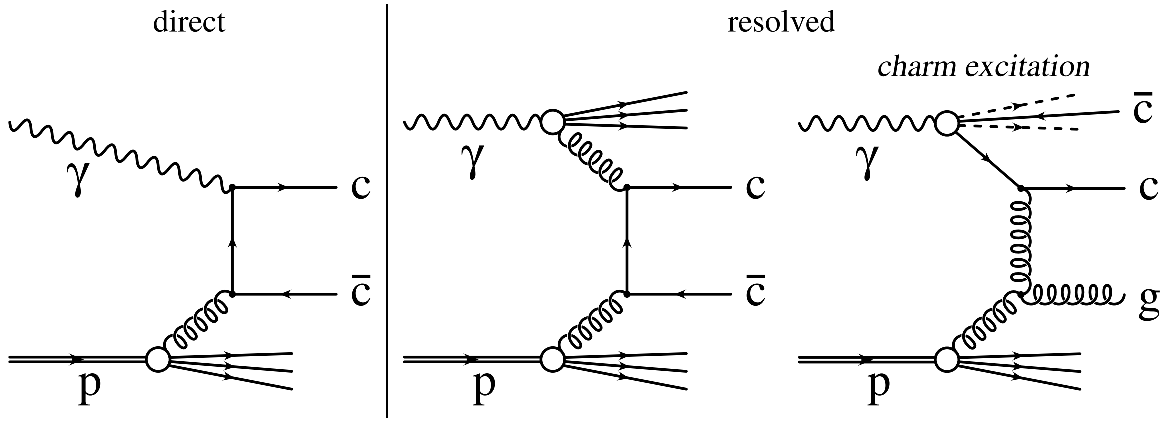

Figure 1: *The main charm production mechanisms in leading order photoproduction: direct and resolved processes where the latter are dominated by charm excitation in the photon.*

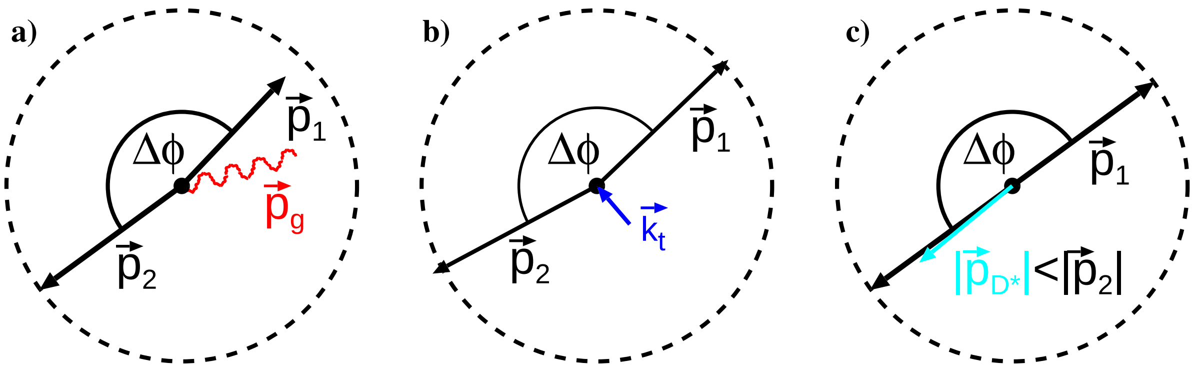

Figure 2: *View perpendicular to the photon-proton direction, illustrating how a radiated gluon with momentum $\vec{p}_g$ (a) or transverse momenta k_t of the incoming partons (b) can lead to a non back-to-back topology of the two outgoing leading hard partons. The momenta $\vec{p}_1$ and $\vec{p}_2$ of these partons would be exactly back-to-back in a $2 \to 2$ process if the incoming partons taking part in the hard interaction collide head-on, like in the collinear factorisation approach. In (c) it is illustrated that the fragmentation of the charm quark with momentum $\vec{p}_2$ into a D^* meson with momentum $\vec{p}_{D^*}$ leads only to a small deviation $\Delta\phi(D^*, jet)$ from $180°$ where the jet is emerging from the parton with momentum $\vec{p}_1$.*

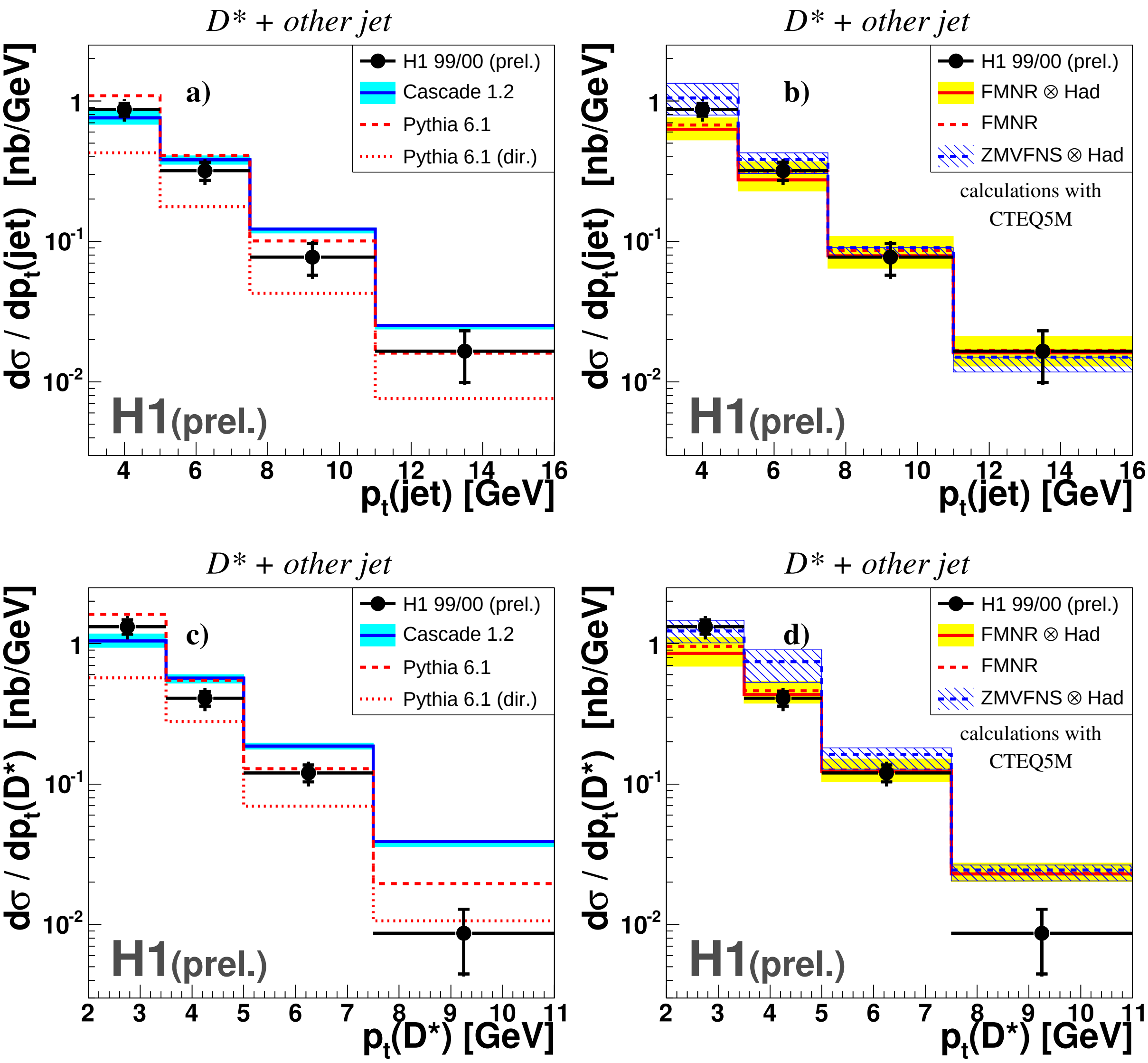

Figure 3: *D^*+jet cross sections in bins of the transverse momentum of the jet and the D^* compared with the predictions of PYTHIA and CASCADE (a,c) and of next-to-leading order calculations (b,d). FMNR is a* massive *and ZMVFNS a* massless *calculation. For PYTHIA the direct contribution of the prediction is shown separately and labelled as* "dir.". *The central FMNR prediction is shown before and after applying the hadronisation corrections.*

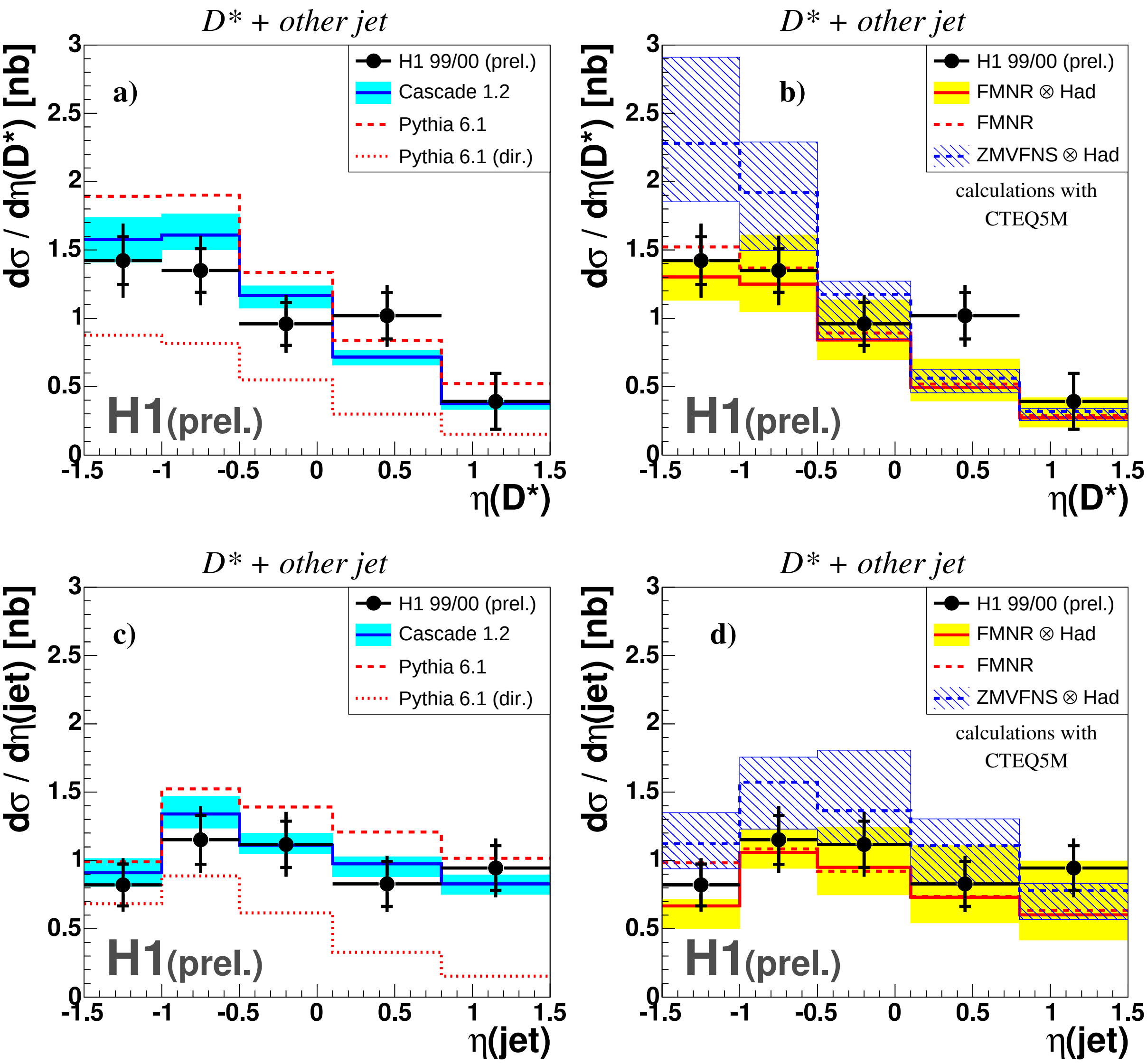

Figure 4: *D^*+jet cross sections in bins of $\eta(D^*)$ (a,b) and $\eta(jet)$ (c,d) compared with the predictions of PYTHIA and CASCADE on the left and of next-to-leading order calculations on the right. FMNR is a* massive *and ZMVFNS a* massless *calculation. For PYTHIA the direct contribution of the prediction is shown separately and labelled as* "dir.". *The central FMNR prediction is shown before and after applying the hadronisation corrections.*

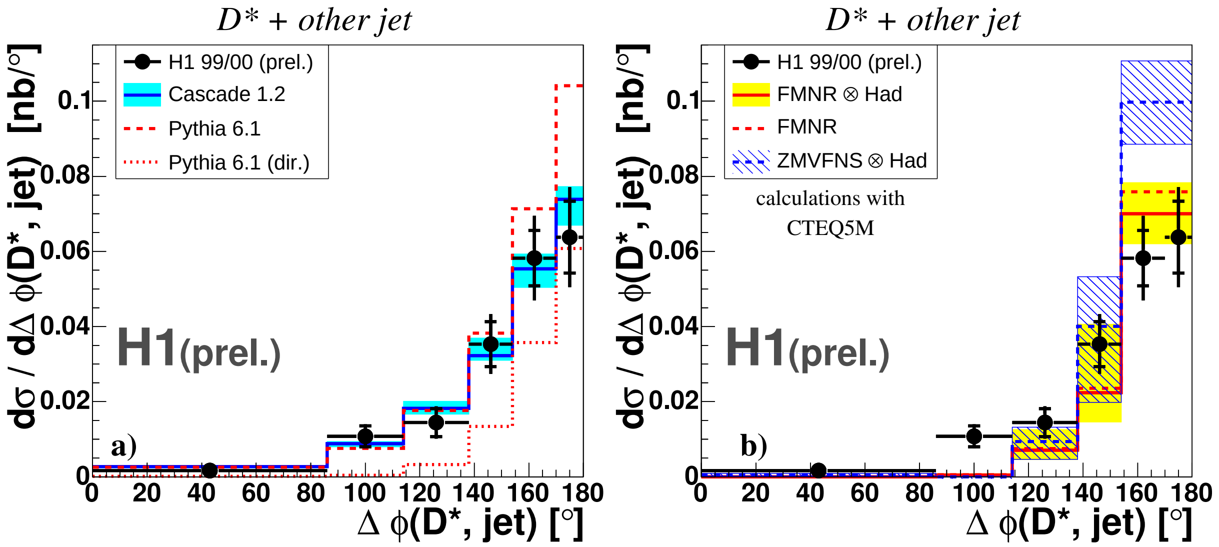

Figure 5: *D^*+jet cross sections in bins of $\Delta\phi(D^*, jet)$ compared with the predictions of PYTHIA and CASCADE on the left and of next-to-leading order calculations on the right. FMNR is a* massive *and ZMVFNS a* massless *calculation. For PYTHIA the direct contribution of the prediction is shown separately and labelled as* "dir.". *The central FMNR prediction is shown before and after applying the hadronisation corrections.*